Supporting Information for:

Controlled Reactions on a Copper Surface: Synthesis and Characterization of Nanostructured Copper Compound Films

Weixin Zhang, Xiaogang Wen, and Shihe Yang*

Department of Chemistry, The Hong Kong University of Science and Technology, Clear Water Bay, Kowloon, Hong Kong

Supporting Information

Contents

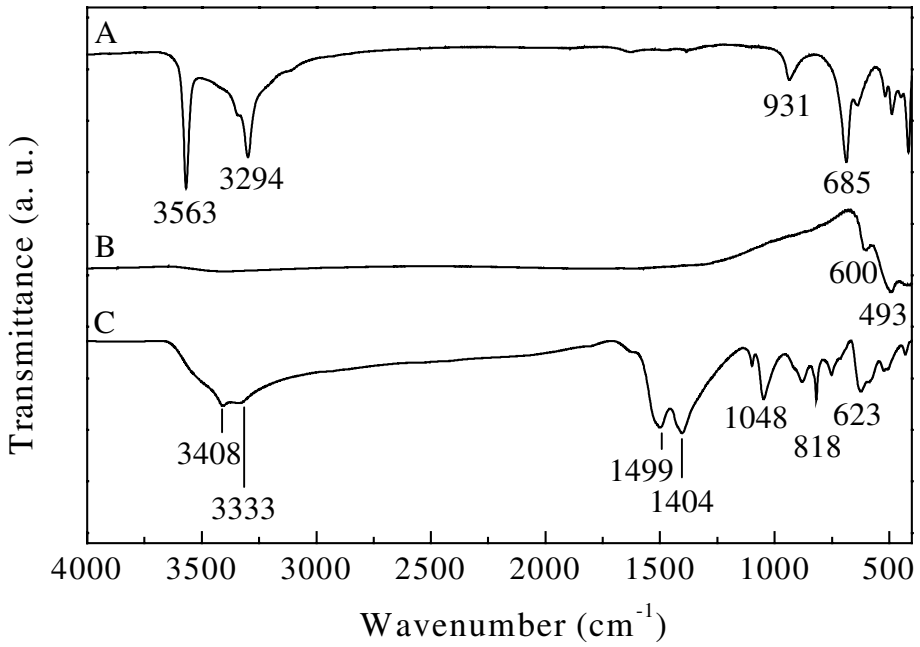

Figure S1. FTIR spectra of different samples oxidized from copper foil: (A) $Cu(OH)_2$ nanofibers (from the same sample as used in Figure 2A); (B) CuO nanosheets/nanowhiskers (from the same sample as used in Figure 2C); and (C) $Cu_2(OH)_2CO_3$ nanorods (from the same sample as used in Figure 2D).

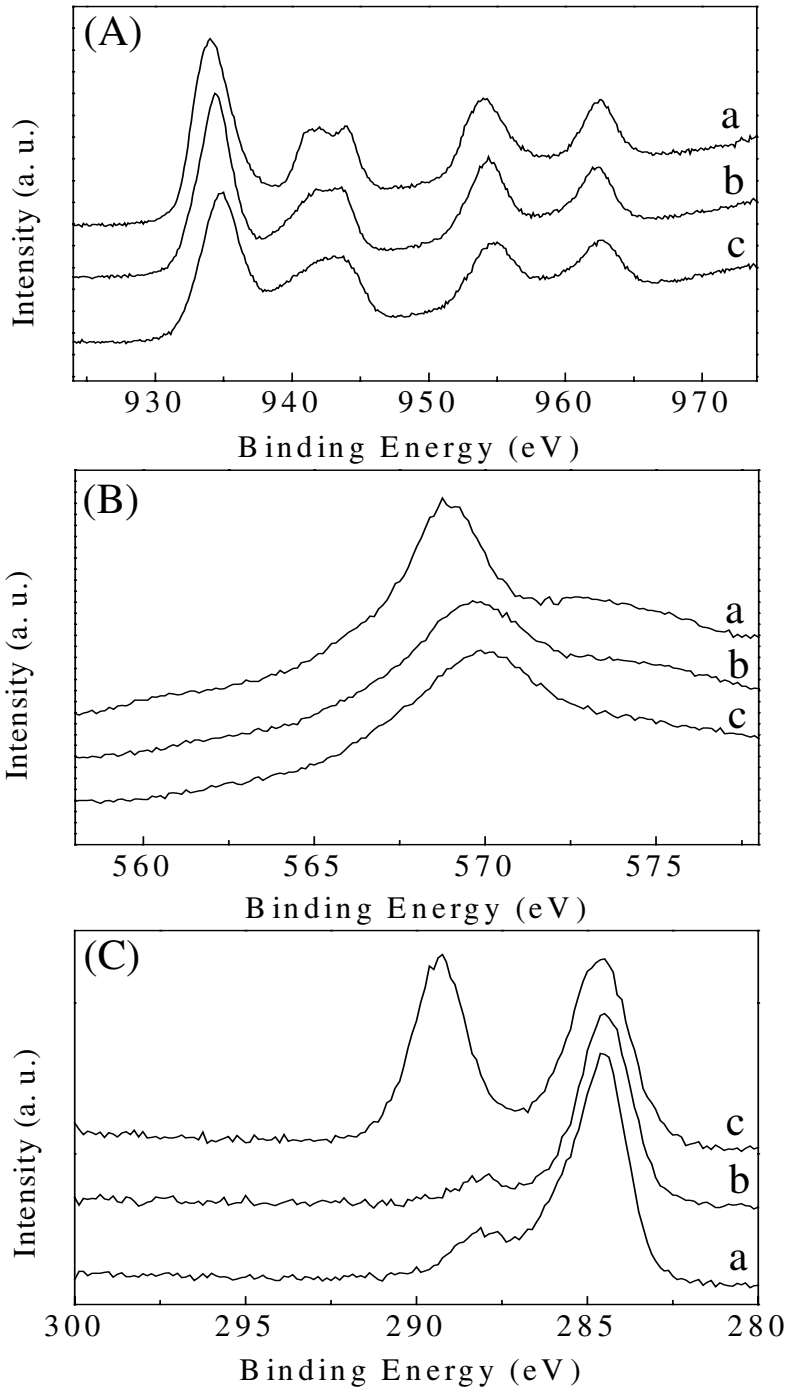

Figure S2. (A) Cu 2p XPS spectra; (B) Cu LMM Auger spectra; and (C) C 1s XPS spectra. Curve a: CuO nanosheets/nanowhiskers (from the same sample as used in Figure 2C); Curve b: $Cu(OH)_2$ nanofibers (from the same sample as used in Figure 2A); and Curve c: $Cu_2(OH)_2CO_3$ nanorods (from the same sample as used in Figure 2D).

Table S1. Observed vibrational modes of the copper compound nanomarterials and their assignments.

Compound	Wavenumber (cm^{-1})	Band (mode)
$Cu(OH)_2$ nanofibers	3563	CuO – H (weaker stretching)
	3294	CuO – H (stronger stretching)
	931	Cu – O (stretching)
	685	Cu – O (bending)
$Cu_2(OH)_2CO_3$ nanorods	3408 ~ 3333	O – H (stretching)
	1499	Carbonate (stretching, γ_3)
	1404	Carbonate (stretching, γ_3)
	1048	Carbonate (stretching, γ_1)
	818	Carbonate (stretching, γ_2)
	752	Carbonate (stretching, γ_4)
	1098	Cu – O (stretching)
	880	Cu – O (stretching)
Cu_2O crystallites	623	Cu – O (bending)
CuO nanosheets	600	Cu – O (stretching)
	493	Cu – O (stretching)

Table S2. Observed XPS (binding energies: eV) and Auger peaks (kinetic energies: eV).

Materials	Cu $2p_{3/2}$	Cu LMM	α'	C 1s	O 1s
CuO nanosheets	934.0	917.8	1851.8	284.5	529.9
$Cu(OH)_2$ nanofibers	934.4	917.0	1851.4	284.5	530.8
$Cu_2(OH)_2CO_3$ nanorods	935.0	916.7	1851.7	284.5, 289.0	531.3

(Kinetic energy of Cu LMM = 1486.6 – Binding energy of Cu LMM; α' = Binding energy of Cu $2p_{3/2}$ + Kinetic energy of Cu LMM)

Infrared absorption spectra. Typical FTIR spectra are shown in Figure S1 and the observed vibrational modes are listed in Table S1. For the $Cu(OH)_2$ nanofibers (Figure S1A), the bands at 3563 and 3294 cm^{-1} are characteristic of the hydrogen bonds, which hold the layers of the distorted $Cu(OH)_6$ octahedra together.[1-3] The IR bands at 931 and 685 cm^{-1} are due to the Cu-O stretching and bending vibrations, respectively.[3] Similar FTIR spectrum was also observed on $Cu(OH)_2$ nanoscrolls. Two bands are observed at 600 and 493 cm^{-1} in the FTIR spectrum of CuO nanosheets (Figure S1B). They can be assigned to the stretching modes of Cu-O.[3,4] The fact that these two bands are not observed in the $Cu(OH)_2$ samples and the CuO-H stretching bands are not observed in the CuO sample indicates the good purity of the intended nanoscale products.

The IR spectrum of the $Cu_2(OH)_2CO_3$ nanorods (Figure S1C) shows five peaks due to the carbonate stretching (Table 3), which are consistent with the data of the corresponding bulk material.[3,5-7] The broad bump around 3408~3333 cm^{-1} is attributed to the O-H stretching. The peaks at 1098 and 880 cm^{-1} are associated with the stretching of Cu-O.[7] A weak band at 623 cm^{-1}, characteristic of crystalline Cu_2O (Cu-O bending), is likely to be due to the presence of small amount of Cu_2O in the $Cu_2(OH)_2CO_3$ nanorod films. However, the amount of Cu_2O may be so small that it escaped the XRD detection.

X-ray photoelectron spectra. The XPS of the nanomaterials in the core level regions of Cu 2p and C 1s have been recorded. The binding energies in the XPS analysis have been corrected for the specimen charging by making reference to the C 1s peak from contaminated carbon at 284.5 eV. Curves a, b, and c in Figure S2A portray, respectively, the Cu 2p XPS spectrum of the black CuO nanosheets, the blue $Cu(OH)_2$ nanofibers, and the deep blue $Cu_2(OH)_2CO_3$ nanorods. The corresponding Cu LMM Auger electron spectra are given in Figure S2B. The Cu $2p_{3/2}$ peaks are located at 934.0 eV (a), 934.4 eV (b), and 935.0 (c), respectively. The Cu (LMM) Auger spectra peak at 568.8 eV (a), 569.6 eV (b), and 569.9 eV (c), respectively. These results verify the existence of Cu^{2+} in the nanostructured films by comparison to the data reported in literature.[8]

Wagner defined a modified Auger parameter (α') as the sum of the binding energy of the most intense photoelectron line and the kinetic energy of the sharpest Auger line, which can be used to distinguish Cu in different oxidation states. This parameter is independent of charging effect

because any shift arising from charging effect is added to the binding energy of the photoelectron line and subtracted from the kinetic energy of the Auger line. The chemical shift in this parameter only reflects changes in screening energy. The α' values of our copper nanomaterials (Table S2) are in good agreement with those of known Cu(II) compounds.[9-11]

Figure S2C shows the C 1s XPS spectra of the nanomaterials. In contrast to the C 1s XPS pattern of CuO (a) and $Cu(OH)_2$ (b) that displays a peak at 284.5 eV with a shoulder at 288.0 eV from contaminated carbon, the C 1s XPS pattern of $Cu_2(OH)_2CO_3$ (c) shows two separate peaks at 284.5 eV and 290.0 eV. These two peaks are attributed to adventitious carbon and carbonate species, respectively.[9] The result verifies the existence of the carbonate group in the $Cu_2(OH)_2CO_3$ nanorod sample.

---

1. (a) Kratohvil S.; Matijević, E. *J. Mater. Res.* **1991**, 6, 766. (b) Rodríguez-Clemente, R.; Serna, C. J.; Ocaña, M.; Matijević, E. *J. Crystal Growth* **1994**, 143, 277. (c) Lee, S. H.; Her, Y. S.; Matijević, E. *J. Colloid Interface Sci*. **1997**, 186, 193.
2. Oswald, H. R.; Reller, A.; Schmalle H. W.; Dubler, E. *Acta Cryst*. **1990**, C46, 2279.
3. Kautek, W.; Geub, M.; Sahre, M.; Zhao, P.; Mirwald, S. *Surf. Interface Anal*. **1997**, 25, 548.
4. Balamurugan, B.; Mehta, B. R. *Thin Solid Films* **2001**, 396, 90.
5. Neufeld, A. K.; Cole, I. S. *Corrosion* **1997**, 53, 788.
6. (a) Monticelli, C.; Fonsati, M.; Meszaros, G.; Trabanelli, G. *J. Electrochem. Soc*. **1999**, 146, 1386. (b) Soler-Illia, G. J. de A. A.; Candal, R. J.; Regazzoni, A. E.; Blesa, M. A. *Chem. Mater*. **1997**, 9, 184.
7. Nyquist, R. A.; Kagel, R. O. *Handbook of Infrared and Raman Spectra of Inorganic Compounds and Organic Salts*; Academic Press: San Diego, **1997**, Vol. 4, p. 85.
8. Cano, E.; Lopez, M. F.; Simancas, J.; Bastidas, J. M. *J. Electrochem. Soc*. **2001**, 148, E26.
9. Chvez, K. L.; Hess, D. W. *J. Electrochem. Soc*. **2001**, 148, G640.
10. Wagner, C. D.; Riggs, W. M.; Davis, L. E.; Moulder, J. F. *Handbook of X-ray Photoelectron Spectroscopy*; Muilenberg, G. E., Ed.; Perkin-Elmer Corporation: Minnesota, **1979**.
11. Deroubaix, G.; Marcus, P. *Surf. Interface Anal*. **1992**, 18, 39.